JP9955059

A Rate-Equation Model for Polarized Laser-Induced Fluorescence to Measure Electric Field in Glow Discharge He Plasmas

K. Takiyama, M. Watanabe and T. Oda
Department of Applied Physics and Chemistry, Faculty of Engineering, Hiroshima University, Higashi-Hiroshima 739, Japan

Possibility of applying polarized laser-induced fluorescence (LIF) spectroscopy for measuring the electric field in a plasma with a large collisional depolarization has been investigated. A rate equation model including the depolarization process was employed to analyze the time evolution of LIF polarization components. The polarized LIF pulse shapes observed in the sheath of a He glow discharge plasma were successfully reproduced, and the electric field distribution was obtained with high accuracy.

1. Introduction

Importance of sheath electric field distribution in discharge plasmas has been well recognized, since it plays an essential role in the charged particle behaviors and in dynamics of the discharge. Several direct measurements have been made in the sheath regions, using laser-induced fluorescence (LIF) techniques [1,2]. In previous reports, we proposed an improved high-sensitive LIF method combined with plasma polarization spectroscopy [3,5]. This method is to observe merely polarization of LIF due to the forbidden excitation of the He metastable atom (2^1S-n^1D) which is caused by the Stark mixing of n^1P to n^1D in the electric field and also by the electric quadrupole moment (QDP), as shown in Fig.1.

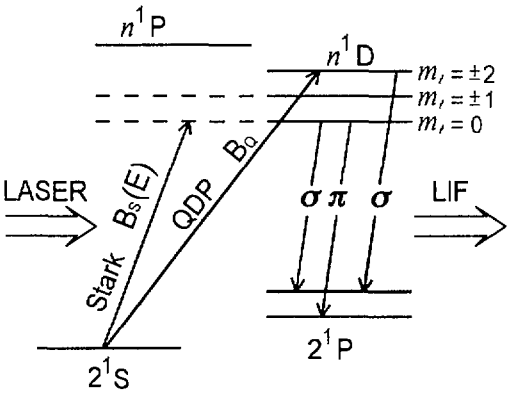

Fig. 1: Partial energy level diagram of HeI and forbidden excitation of metastable atoms by laser polarized linearly parallel to the electric field without magnetic field, relevant to the polarized fluorescence.

The excited atoms decay with intense allowed fluorescence (n^1D-2^1P). The intensity I_F is written as a function of electric field strength E as follows:

$$I_F \propto n_{2S}\rho_L[B_S(E)+B_Q] , \qquad (1)$$

where ρ_L is a laser power density, n_{2S} is the metastable atom density, $B_S(E)$ is the absorption coefficient for the Stark transition ($B_S(E) \propto E^2$), and B_Q is the absorption coefficient for the QDP transition. The observed fluorescence is usually polarized,

because anisotropic population between sublevels in the excited states (alignment) is achieved with the linearly-polarized laser excitation [6]. The polarization of the Stark component is quite different from that of the QDP (for example, see Fig. 1) [3]. Considering the alignment and the selection rules for the allowed transition (n^1D-2^{1}P), the ratio $B_S(E)/B_Q$ is a function of the polarization degree P in a given observation geometry and the electric field is simply described in the following:

$$E = C\sqrt{B_S(E)/B_Q} = C\sqrt{f(P)}\,. \qquad (2)$$

Here, C is the electric field strength at $B_S(E)=B_Q$, which can be quantum-mechanically calculated. When the laser polarization e_L is parallel to the z-axis in our observation geometry (see section 3), f(P) in two cases without magnetic field and with magnetic field are simply given by $6P/(3\text{-}5P)$ and $(3\text{-}9P)/(10P\text{-}6)$, respectively.

In plasmas with higher particle density (electrons, ions and atoms), however, the decay of polarization becomes faster and the LIF waveform is considerably modified by the frequent collisions of the aligned n^1D atoms with the plasma particles (collisional depolarization). In such cases it will become difficult to estimate E straightforwardly from the experimental P. To evaluate E accurately, we analyze temporal evolution of polarized LIF by using a rate-equation model involving the depolarization process of aligned atoms in this report. Specifically, the following factors determine the waveform: De-population of n^1D states, collisional transfer between magnetic sublevels in n^1D states (disalignment), laser pulse profile, and time response of detection system. All of these should be included in the model.

2. Rate-equation model

We assume that polarization decay is caused by the collisional transfers between three Stark sublevels m_ℓ of n^1D state specified by magnetic quantum numbers 0, ±1 and ±2, respectively, as shown in Figs. 1, 2. The rate coefficients for collisional transfers from m_ℓ to m_ℓ', $R(m_\ell, m_\ell')$, are defined considering the detailed balance in the following:

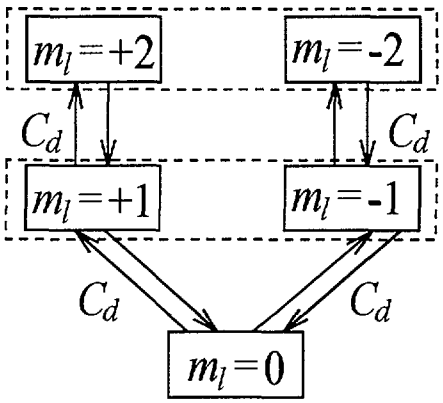

Fig. 2: Three Stark sublevels in n^1D state and collisional depolarization mechanism.

$$
\begin{aligned}
&R(0,\pm1) = 2C_d,\\
&R(\pm1,0) = C_d,\\
&R(\pm1,\pm2) = C_d,\\
&R(\pm2,\pm1) = C_d.
\end{aligned}
\qquad (3)
$$

Here, C_d denotes the transfer rate between adjacent Zeeman sublevels, as shown in Fig.2. The temporal evolution of the population density $n_{m_\ell}(t)$ of a sublevel m_ℓ in n^1D level can be written as a set of rate-equations:

$$
\begin{aligned}
\frac{dn_{m_\ell}}{dt} &= -n_{m_\ell}\left(\sum_{k<m_\ell} A_{m_\ell k} + \sum_k n_{e,a}\langle\sigma_{e,a}v\rangle_{m_\ell k} + \sum_{m_\ell'} R(m_\ell, m_\ell')\right)\\
&+\left(\sum_{k>m_\ell} n_k A_{k m_\ell} + \sum_k n_k n_{e,a}\langle\sigma_{e,a}v\rangle_{k m_\ell}\right) + \sum_{m_\ell'} n_{m_\ell'} R(m_\ell', m_\ell) \qquad (4)\\
&+ I_{\ell m_\ell}(t)(n_\ell B_{\ell m_\ell} - n_{m_\ell} B_{m_\ell \ell}),
\end{aligned}
$$

where $A_{m_\ell k}$ is the radiative transition probability from level m_ℓ to level k, $n_{e,a}$ is the electron or atom density, $\langle\sigma_{e,a}v\rangle_{m_\ell k}$ the excitation or de-excitation rate coefficient by electron or atom impact. The last term on the right-hand side corresponds to laser pumping of 2^1S to m_ℓ, where $B_{\ell m_\ell}$ is the absorption coefficient in the forbidden transition ($\ell \rightarrow m_\ell$).

By solving numerically a set of rate equations for each levels from n=1 to 6 with the Runge-Kutta method, the temporal behaviors of population are obtained. Parallel and perpendicular components of LIF ($I_{//Z}$ and $I_{\perp Z}$) are reconstructed from the calculated sublevel populations of n^1D considering the quantization axis, the selection rules of the transition from the sublevels of n^1D to those of 2^1P, and also the instrumental time response function. Then, the time evolution of LIF polarization is given by

$$
P(t) = \frac{I_{//Z}(t) - I_{\perp Z}(t)}{I_{//Z}(t) + I_{\perp Z}(t)}. \qquad (5)
$$

3. Experimental

The observation geometry is shown in Fig. 3. The plasma was produced in helium gas between a pair of plane-parallel disk electrodes (diameter of 4 cm and separation of 1 cm) with discharge voltage of 1 kV and current of 15 mA at gas pressure of 2 Torr. The z-axis was taken to be perpendicular to the electrode surface, i.e., parallel to the electric field in the sheath, and its origin was the center of the gap. An electric probe measurement showed that almost all the

discharge voltage was applied over the dark space with width of ~6 mm and the electron temperature and density were ~1 eV and ~1x10^{11} cm^{-3}, respectively, at the center of the negative glow when B=0.

A laser beam exciting the forbidden transition (2^{1}S-3^{1}D, 504.2 nm) with pulse width of 5 ns was injected into the plasma along the y-axis, and the polarized LIF (3^{1}D-2^{1}P, 667.8 nm) was observed along the x-axis. Spatial distribution of LIF was measured by scanning the plasma vessel along the z-axis.

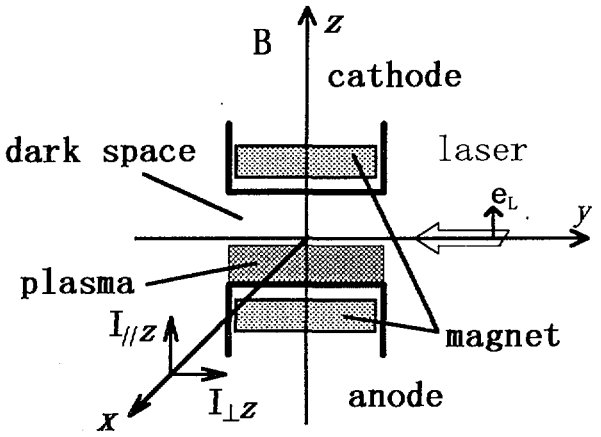

Fig. 3: Geometry of LIF observation and the cross section of glow discharge vessel

4. Results and Discussion

Polarization components of 667.8 nm fluorescence (3^{1}D-2^{1}P) , $I_{//z}$ and $I_{\perp z}$, induced by laser with $e_L \perp z$ were observed at the plasma region (z=−1mm) in the vicinity of the sheath, where only the QDP transition occurs, since the electric field is negligibly small, as shown in Fig 4 (a). Using eq. (5) temporal polarization P obtained from experimental $I_{//z}$ and $I_{\perp z}$ is depicted by open circles in Fig. 4 (b). The polarization at the earlier stage is ~−0.8 very close to unity, reflecting a feature of polarized LIF due to the QDP excitation. Since the quantization axis for QDP excitation is always perpendicular to the polarization plane of laser without magnetic field, the direction turns to z-axis and the atoms are selectively excited to the sublevels m_ℓ=±2 in 3^{1}D [3]. Excited atoms subsequently decay down to the 2^{1}P state with allowed σ-fluorescence of 667.8 nm. We are supposed to observe perfectly negative polarization of the fluorescence in our

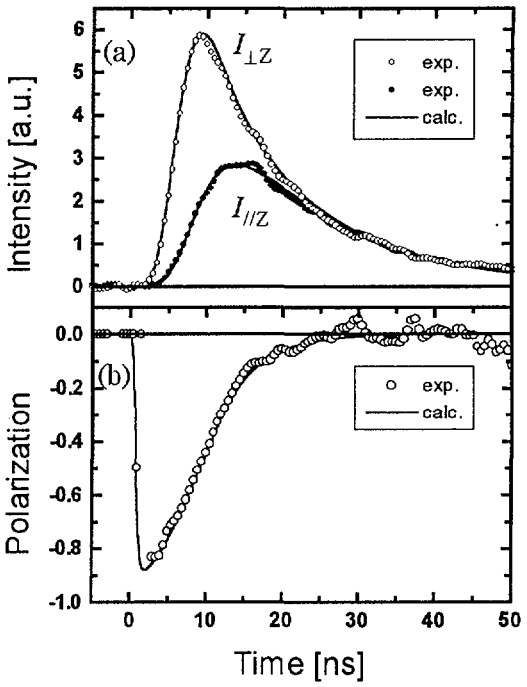

Fig. 4: Calculated waveforms fitted to the experimental ones observed by laser excitation ($e_L \perp z$) at the negative glow region.

geometry. However, considerable depolarization due to collisional disalignment was observed. The disalignment and de-population rates are estimated to be 2.1×10^8 s^{-1} and 0.7×10^8 s^{-1}, respectively, from the slopes of semi-logarithmic plots of time evolution of longitudinal alignment and population.

In our fitting procedure between the calculated curves with the experimental LIF ones (open and closed circles in Fig. 4), we took the transfer rate (C_d) as a fitting parameter. When $C_d = 1.5\times10^8$ s^{-1}, the best-fit curves of $I_{//Z}$, $I_{\perp Z}$ and P were obtained, as represented by solid lines in Fig. 4 (a), (b).

Figure 5 (a) shows polarization components $I_{//Z}$ and $I_{\perp Z}$ of LIF observed at z=4mm in the sheath region under excitation by laser with $e_L//z//E$. The temporal polarization is also depicted by open circles in Fig. 5 (b). In the sheath electric field a polarized laser simultaneously excites both Stark and QDP transitions. The quantization axis for Stark excitation can be taken to the direction of electric field ($//z$) independently to the laser polarization and the value of P is always positive. On the other hand QDP component is unpolarized in this excitation geometry. Remarkable positive value of P at the earlier stage shows that in LIF the Stark component is dominantly included rather than the QDP one: Most of excited atoms populate in the sublevel m_ℓ=0 in 3^1D. The disalignment and de-population rates estimated in the similar way described above were the same values as ones obtained at z=−1mm in the plasma region near the sheath. This means that C_d as well as plasma parameters are almost the same in the observed region from z=−1 mm to cathode. Using C_d obtained above, we can determine uniquely the electric field E by fitting the calculated curves to the experimental ones observed in the sheath region. The best-fit curves, solid curves in Fig.5 (a), (b), are obtained when E=2.7kV/cm.

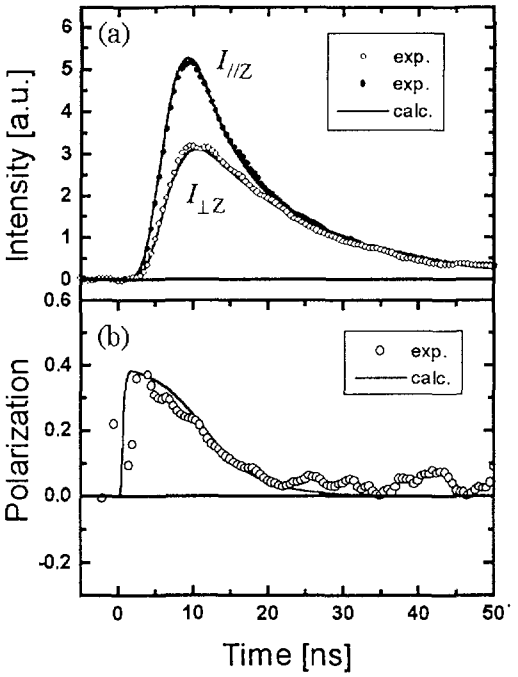

Fig. 5: Calculated waveforms fitted to the experimental ones observed by laser excitation ($e_L//z$) at the sheath region.

For the case of B=200G, same procedures are also carried out to reconstruct the polarized LIF.

Spatially resolved LIF signals were obtained by scanning the plasma vessel. Using the same procedure as described above, spatial profiles of E in the sheath region of both plasmas with B=0 and B=200 G were obtained as shown in Fig. 6, in which electric field is increasing linearly toward the cathode surface. From the profiles, sheath thickness d and cathode-fall potentials V_C were obtained, as presented in Table I with experimental conditions. It should be noted that the potentials for both cases are in good agreement with one obtained by the electric probe. The proportionality between the transfer rate C_d and the He gas pressure suggests that the strong depolarization process is dominantly caused by collisions of aligned 3^1D atoms with ground state He atoms for the present cases.

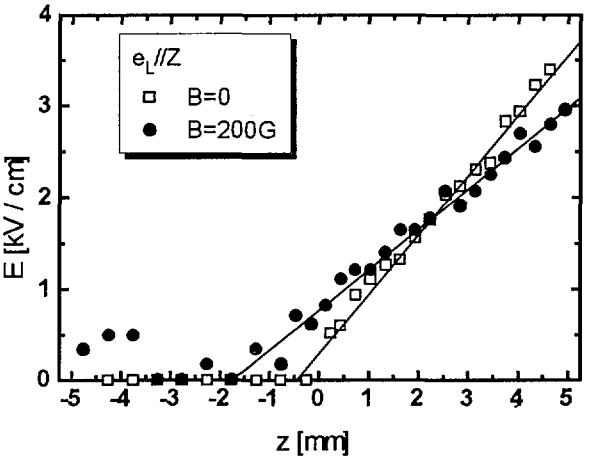

Fig. 6: Spatial distribution of electric field

Thus, the polarized laser-induced fluorescence spectroscopy was successfully applied to measure the electric field profiles in the sheath of the plasma with higher He gas pressure and of magnetized plasma with the aid of the rate-equation analysis. The sensitivity of this method is increased by exciting the higher n level. At n=5, the electric field of a few tens V/cm can be measured.

Table I Summary of the LIF and electric probe measurements

	Discharge condition			LIF			Electric probe
	He Pressure (Torr)	Discharge current (mA)	Magnetic field B(G)	Transfer rate $C_d(s^{-1})$	Sheath thickness d(mm)	Cathode-fall potential V_C(kV)	Cathode-fall potential V_C(kV)
(a)	3	15	0	1.5×10^8	5.6±0.2	1.03±0.05	1.0
(b)	2	15	200	1.0×10^8	6.9±0.5	1.06±0.10	1.0

Acknowledgements

This work was supported in part by a Grant-in-Aid for Scientific Research (C) from the Ministry of Education, Science, Sports and Culture, and by Electric Technology Research Foundation of Chugoku.

References

[1] H. Sakai, K. Takiyama, et al., J. Nucl. Mater. 196-198 (1992) 1135.

[2] M. D. Bowden, Y. W. Choi and K. Muraoka, Appl. Phys. Lett. 66 (1995) 1059.

[3] K. Takiyama, et al., *Proc. 6th Int. Sympo. Laser- Aided Plasma Diagnostics,* Bar Harbor, Maine, Oct. 25-28, 1993, p.43.

[4] T. Oda and K. Takiyama, *Proc. 7th Int. Sympo. Laser-Aided Plasma Diagnostics*, Fukuoka, Dec. 5-8, 1995, p.227.

[5] K. Takiyama et al., Rev. Sci. Instrum. 68 (1997) 1028.

[6] T. Fujimoto and A. Kazantsev, Plasma Phys. Control. Fusion 39 (1997) 1267